Results in Chemistry 3 (2021) 100242

Contents lists available at ScienceDirect

Results in Chemistry

journal homepage: www.sciencedirect.com/journal/results-in-chemistry

Chemical and Cytotoxic Activity of three main Sesquiterpenoids from *Warburgia ugandensis*

Reni Kitte [a,1], Maik Tretbar [b,1], Sarah Dluczek [a], Lorenz Beckmann [b], Peter Marquardt [c], Anna Duenkel [a], Andreas Schubert [d], Stephan Fricke [a,2], U. Sandy Tretbar [a,2,*]

[a] Department of GMP Process Development/ATMP Design, Fraunhofer Institute for Cell Therapy and Immunology IZI, Perlickstr. 1, 04103 Leipzig, Germany
[b] Institute for Drug Development, Medical Faculty, University of Leipzig, Bruederstr. 34, 04103 Leipzig, Germany
[c] Department of Pharmaceutical Biology, Medical Faculty, University of Leipzig, Johannisallee 21-23, 04103 Leipzig, Germany
[d] Department of Immunology, Fraunhofer Institute for Cell Therapy and Immunology IZI, Perlickstr. 1, 04103 Leipzig, Germany

ARTICLE INFO

Keywords:
Warburgia ugandensis
Sesquiterpenoids
Natural products isolation
Cytotoxicity
Cancer

ABSTRACT

Plant materials of *Warburgia ugandensis* have long been used in traditional African medicine due to their broad spectrum of biological activity. Here, we describe an efficient and mild isolation of three major compounds polygodial **1a**, warburganal **2a**, and muzigadial **2b** using Soxhlet extraction and combined preparative separation methods. Furthermore, 9-deoxymuzigadial was reported for the first time from this species. Since *in silico* analysis predicted drug-likeness, the compounds were tested against leukemia and solid cancer cell lines as well as human primary cells *in vitro*. The most susceptible cells were THP-1 indicating a selective effect against monocytes pointing towards a potential treatment of monocytic leukemia. The most robust cells were primary gingival fibroblasts offering selectivity also to solid cancers. The results in this study shed new light on long-known chemical compounds from traditional medicine and pave the way for *in vivo* studies to advance the substances to the next level towards the use as anti-cancer drugs.

Introduction

According to the World Health Organization, cancer is currently one of the major health challenges facing the world [1] and ranks as the most common cause of death in the 21st century [2]. In 2020, 9.96 million deaths were reported, which is expected to increase to 16.3 million deaths by 2040 [3]. To combat this growing issue, screening of natural biomass sources is a promising approach in the development of innovative anti-cancer drugs. Previously, natural products have often played an important role in the search for new drugs and lead structures for active ingredients [4]. Therefore, the selection of plants as a source for novel therapeutics is an appropriate strategy since plants naturally produce a wide range of secondary metabolites [5].

In traditional African medicine, *Warburgia ugandensis* is highly valued and frequently used to treat a wide range of diseases [6]. In fact, in several phytochemical studies, antibacterial [7–9], antifungal [8,9], antiparasitic [10,11] as well as antioxidant [12] and cytotoxic [9] activities were reported for *W. ugandensis* extracts. Interestingly, compared to other members of evergreen native tree species, *W. ugandensis* extracts had an oral $LD_{50} > 5000$ mg/kg body weight in mice, and no mortality was recorded in dose levels ranging from 500 to 5000 mg/kg body weight indicating safety for human use [13].

In the extracts of stem bark, drimane- and coloratane-type sesquiterpenoids were identified including the three major biologically active compounds polygodial **1a**, warburganal **2a**, and muzigadial **2b** [6,14–16] (Fig. 1) together with other known oxo-functionalized drimane-type sesquiterpenoids mukaadial and ugandensidial [17]. Other drimane-type sesquiterpenoids such as 9-epi-polygodial [46], drimenol, drimenin [47], pereniporin B, cinnamolide, cinnamolide-3β-acetate, deacetylugandensolide [6], and dendocarbin A [18] were observed in the analyzed bark extract. The coloratane-type sesquiterpenoids, the rearranged bicyclic drimane-type ones, muzigadiolide, 11α-hydroxy

Abbreviations: GF, gingival fibroblasts; IC_{50}, half-maximum inhibitory concentration; PBMC, peripheral blood mononuclear cells; PS, phosphatidylserine; RF, relevant fraction; ROS, reactive oxygen species; SI, selectivity index; TRPV1, transient receptor potential vanilloid-1.

* Corresponding author.
E-mail address: sandy.tretbar@izi.fraunhofer.de (U.S. Tretbar).
[1] These authors contributed equally.
[2] These authors share equally last authorship.

https://doi.org/10.1016/j.rechem.2021.100242
Received 9 September 2021; Accepted 8 November 2021
Available online 11 November 2021

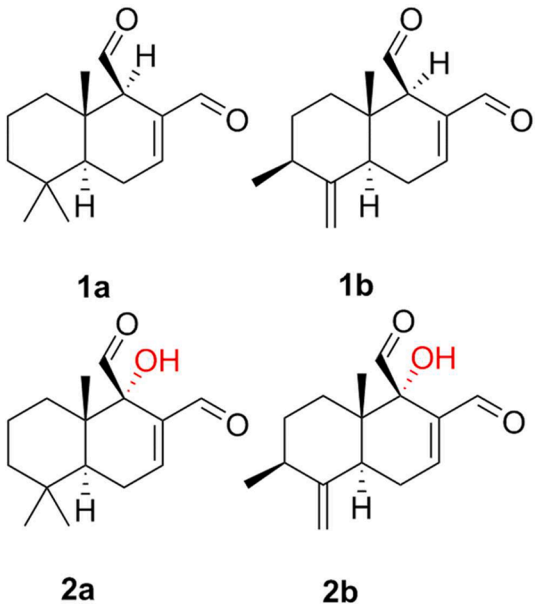

Fig. 1. Chemical structures of the sesquiterpenoids polygodial **1a**, 9-deoxymuzigadial **1b**, warburganal **2a**, and muzigadial **2b**.

muzigadiolide, and 7α-hydroxy-8-drimen-11,12-olide have also been reported as compounds in the stem bark of *W. ugandensis* [17] (Fig. S1 in Supporting Information).

The path of natural product extraction to the pure target compounds requires many time-consuming steps. In this work, we present an isolation strategy using mild extraction conditions for effective and reproducible isolation of **1a**, **2a**, and **2b** from *W. ugandensis* stem bark. Furthermore, the drug-likeness was investigated using the *in silico* prediction tool SwissADME. In order to derive new applications in human health care, the extract, relevant fractions as well as the isolated compounds were tested against different human cancer cell lines *in vitro*. This study brings already known compounds into new spotlight as potential anti-cancer therapeutics and highlights a new model for a possible mechanism of action.

Results and discussion

Efficient isolation of three sesquiterpenoids in one process

By a process coupling a mild Soxhlet extraction and two combined flash column chromatographies (for detailed description see chapter 2 in Supporting Information), three sesquiterpenoids identified as polygodial **1a**, warburganal **2a**, and muzigadial **2b** (chapter 3 in Supporting Information) were efficiently isolated from *W. ugandensis*. In this process, ground stem bark material (30 g) was extracted for 5 h using dichloromethane (350 mL). The solvent was evaporated leaving the extract (3.58 g, 11.93 wt%), which was fractionated by CombiFlash® chromatography. Fractions eluted between 7.1 and 8.3 min were combined and concentrated providing the relevant fraction 1 (RF1; 390 mg, 1.30 wt%). Fractions eluted between 8.3 and 10.4 min were combined and concentrated providing relevant fraction 2 (RF2; 591 mg, 1.97 wt%) (Fig. S3 in Supporting Information). RF1 and RF2 were fine purified by a second flash chromatography to obtain polygodial **1a** (191 mg, 0.64 wt %) from RF1 as well as warburganal **2a** (322 mg; 1.07 wt%) from RF2. Additionally, after a longer bark storage time, 9–deoxymuzigadial **1b** (44 mg, 0.15 wt%) was found in RF1 in NMR analyses in less concentration (**1a** = 0.52 wt%; **1b** = 0.15 wt% yield) while muzigadial **2b** (226 mg, 0.75 wt%) was obtained from RF2 in higher concentration (**2a** = 0.02 wt%; **2b** = 0.75 wt%). However, the similar polarity of **1a** and **1b** as well as **2a** and **2b** resulted in separation issues for initial purification steps.

The isolation process was monitored by thin layer chromatography and high performance liquid chromatography. Thereby, the compounds **1a**, **2a**, and **2b** were continuously detected (Table 1, Fig. S4 in Supporting Information) allowing a straightforward purification and isolation. Based on the currently available literature, **1b** is reported for the first time as a compound of *W. ugandensis*. Previously, **1b** was isolated only from species of other genera such as *Pseudowintera* and *Canella* [20,21].

The isolation process was completed within three days including two overnight drying steps. The rapidness of the extraction method reflects its high efficiency. Here, Soxhlet extraction with dichloromethane already yielded 7 wt% extract within one extraction cycle (about 1 h), which could be improved to about 12 wt% by increasing the number of cycles (extraction time) (Fig. S5 in Supporting Information). In comparison to studies which performed dichloromethane maceration, only 4 wt% and 5 wt% extract yields were obtained after 48 h and 72 h [22,23]. Moreover, using maceration, solid plant parts must be removed from the extract which can complicate the procedure [24]. The process presented here including Soxhlet extraction is not affected by this particular difficulty, since the solid plant material is efficiently excluded from the extract by the extraction thimble. However, although Soxhlet extraction is not suitable for thermolabile compounds compared to maceration [25], the use of dichloromethane, which has a low boiling point of 40 °C under normal pressure, allows a mild extraction at a relatively low temperature. Moreover, Soxhlet extraction is an automatic, continuous method and still consumes only small amounts of solvent [25]. Thus, the mild Soxhlet extraction described here is not only very efficient, but also sustainable regarding solvent consumption.

Since this study focused on an efficient isolation, stem bark instead of leaves was chosen as starting material for extraction as higher extract yields were obtained from stem bark material than from leaves (Fig. S5 in Supporting Information). Furthermore, for the stem bark extract, a higher number of intense spots not originating from chlorophyll and other photosynthetic molecules were detected on thin layer chromatography plates indicating higher concentrations of extracted secondary plant metabolites including the compounds **1a**, **1b**, **2a**, and **2b** (Fig. S6 in Supporting Information). In fact, it was reported that *W. ugandensis* stem bark extracts were more bio-active than extracts from leaves [7].

Interestingly, it was observed that the heights of the peaks representing compounds **1a**, **2a**, and **2b** in the extract's high performance liquid chromatogram changed over storage time of the stem bark. For compound **2b**, the peak height in the chromatogram of freshly ground stem bark was increased compared to that of ground stem bark from the same plant but stored for 1 year. In contrast, the peak heights representing compounds **1a** and **2a** declined with longer storage time of the ground stem bark (data not shown). From these observations, it can be assumed that drimane sesquiterpenoids such as **1a** and **2a** are less stable in ground *W. ugandensis* stem bark than coloratanes like **2b**. Based on these results, the choice of the explicit stem bark material depends on the target compound; its degradation in the raw material should therefore be investigated to guarantee an effective and sustainable isolation process regarding the starting material.

Drug-likeness prediction

Structure-related physicochemical parameters and absorption, distribution, metabolism, and excretion (ADME) properties were evaluated to predict the drug-likeness of **1a**, **1b**, **2a**, and **2b** using the free web tool SwissADME [26]. All four compounds were predicted to exhibit favorable properties regarding oral bioavailability, gastrointestinal absorption, skin permeability as well as metabolic elimination and thus rated as drug-like, which was already reported for **2b** [23] (for detailed data and discussion see chapter 5 and Table S3 in Supporting Information).

Table 1
Characteristics of the compounds **1a**, **1b**, **2a**, and **2b** during the isolation process.

Analysis	Specification[a]	Key figure	RF1		RF2	
			1a	1b	2a	2b
CombiFlash® CC	Silica phase, CH:EA gradient	Elution time [min]	7.1–8.3	7.1–8.3	8.3–10.4	8.3–10.4
TLC	Silica phase, CH:EA = 4:1	R_f [-]	0.24	0.24	0.17	0.17
TLC	Silica plate, CH:EA = 3:2	R_f [-]	0.62	0.62	0.53	0.53
HPLC	C_{18} phase, water:ACN gradient	t_R [min][b]	17.58	17.60	15.18	14.93
GC–MS	Electron ionization	t_R [min]	7.38	7.40	7.44	7.45
ESI-MS	ESI positive; time-of-flight	M_{found} [g/mol]	234	232	250	248
Mass balancing	of RF	Yield [mg][c]	390		591	
		Yield [wt%]	1.30		1.97	
		Change during bark storage	↓		↓	
	of the compounds derived from fresh bark material	Ratio	95.5	4.5	77.5	22.5
		Yield [mg][c]	191	9[d]	322	94[d]
		Yield [wt%]	0.64	0.03[d]	1.07	0.31[d]
	of the compounds derived from stored bark material (1 year)	Ratio	78.0	22.0	2.0	98.0
		Yield [mg][c]	156[e]	44[e]	5[d]	226
		Yield [wt%]	0.52[e]	0.15[e]	0.02[d]	0.75

[a] Detailed description in Supporting Information. [b] corrected to internal standard. [c] from 30 g ground bark material. [d] theoretically determined. [e] theoretically determined assuming 200 mg of **1a** + **1b**.
Abbreviations: ACN, acetonitrile; CC, column chromatography; CH, cyclohexane; EA, ethyl acetate; ESI-MS, electrospray ionization – mass spectrometry; GC–MS, gas chromatography – mass spectrometry; HPLC, high performance liquid chromatography; RF1/RF2, relevant fraction 1/2; R_f, retention factor; TLC, thin layer chromatography, t_R, retention time.

Cytotoxicity against hematopoietic cells

After their use as antibiotics for infectious diseases, herbal agents became more and more relevant as therapeutics with anti-cancer properties. In this context, **1a** and derivatives thereof were recently shown to exhibit cytotoxic activity against hematopoietic cell lines e.g. K-562 (chronic myeloid leukemia) and Nalm-6 (acute B lymphoblastic leukemia) [27]. With regard to these results, in the present study, the extract, RF1, RF2, and the compounds **1a**, **2a**, and **2b** were tested against non-malignant peripheral blood mononuclear cells (PBMC) as well as against the blood cancer cell lines MV4-11 (biphenotypic B myelomonocytic leukemia) and THP-1 (acute monocytic leukemia) *in vitro*. The treatment with 1% Triton X-100 served as positive control representing the maximum cell lysis effect to be reached by our test compounds. All test materials led to significantly decreased cell viabilities at 100 µg/mL (Fig. 2**A**) indicating a strong cytotoxic effect at this concentration. Since **1b** was only found in NMR analysis but could not be isolated as pure substance, it was not possible to test its cytotoxic activity so far.

To evaluate a selective anti-cancer activity of **1a**, **2a**, and **2b**, the respective selectivity index (SI) defined as the quotient of the toxic

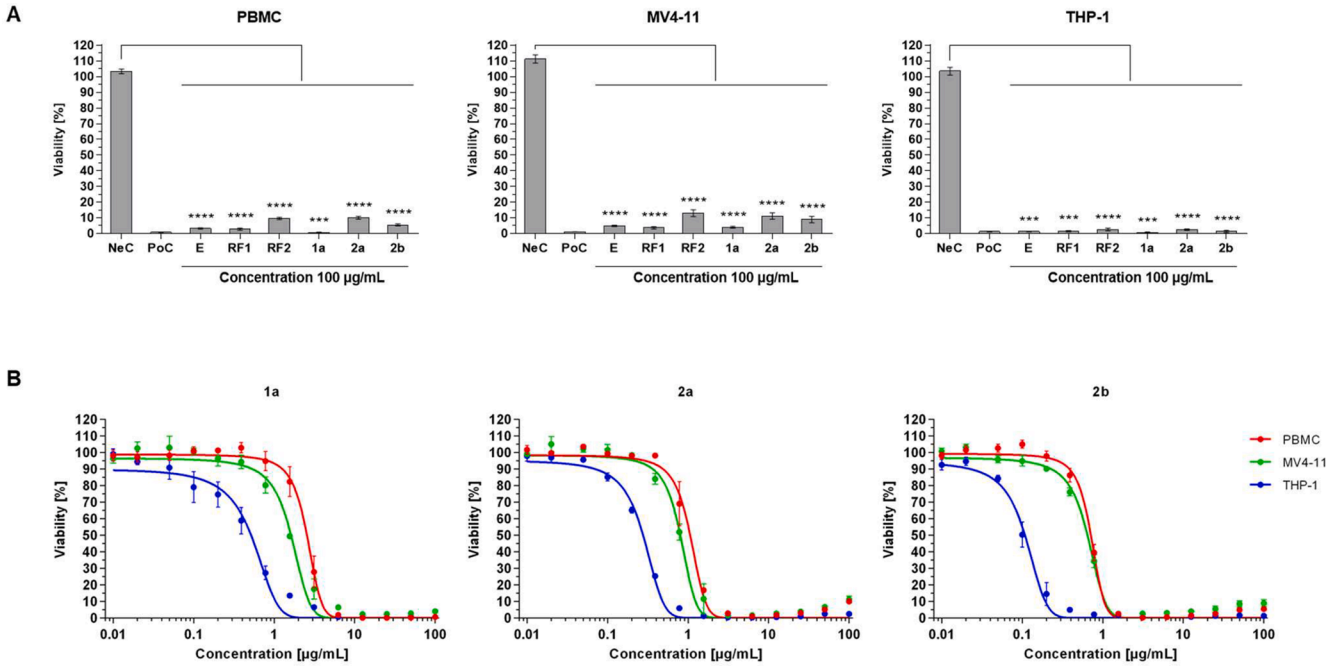

Fig. 2. Effects of *W. ugandensis* plant materials and its single compounds on the viability of human hematopoietic cells. **A)** 100 µg/mL of the extract (E), relevant fractions 1 (RF1) and 2 (RF2), **1a**, **2a**, and **2b**, respectively, were tested against non-malignant human peripheral blood mononuclear cells (PBMC) as well as the cancer cell lines MV4-11 and THP-1. 1% Triton X-100 was used as positive control (PoC) indicating complete cell lysis. Cell viabilities were compared to those of untreated cells (negative control, NeC) (*** $p < 0.001$; **** $p < 0.0001$ (unpaired *t*-test with/without Welch's correction)). **B)** Dose-response curves of **1a**, **2a**, and **2b** against PBMC, MV4-11, and THP-1. Cell viabilities were normalized to viability of untreated cells. Non-linear regression was used to display sigmoidal curves of the cell viability allowing the determination of the respective half-maximum inhibitory concentration (IC_{50}). The experiments were performed in triplicates including three biological replicates with three technical replicates each, and the data are expressed as arithmetic mean ± standard error of the mean indicated by error bars.

concentration against non-malignant cells and the effective concentration against malignant cells was calculated. Therefore, dose–response curves were recorded to determine the half-maximum inhibitory concentration (IC_{50}) of the compounds (Fig. 2**B**). The IC_{50} values of the test materials against MV4-11 ranged from 0.65 μg/mL (2.62 μM of compound **2b**) to 1.62 μg/mL (6.91 μM of compound **1a**), which were comparable to the IC_{50} results against PBMC leading to SI around 1 (Fig. 2**B**, Table 2.). Generally, a SI > 10 shows high selectivity of a compound, which could hence serve as a therapeutically useful substance [28]. Thus, the test materials were assumed not to be selective to biphenotypic B myelomonocytic leukemia cell line. In contrast, THP-1 cells were the most susceptible cells with IC_{50} values between 0.11 μg/mL (0.44 μM of compound **2b**) and 0.52 μg/mL (2.22 μM of compound **1a**) and SI between 3.79 (compound **2a**) and 6.45 (compound **2b**). Although the test materials were not fully selective to acute monocytic leukemia cells, the results indicate a selective effect on monocytic cells. Indeed, it was observed that, at the respective IC_{50}, PBMC completely lack $CD14^+$ cells representing monocytes. In contrast, $CD3^+$, $CD19^+$ and $CD56^+$ cells representing T, B, and natural killer cells were still detected with comparable percentages as PBS treated cells (Figure S8 in Supporting Information). This indicates that the strong decrease of PBMC viability was most likely due to the inhibition of the monocyte population. As a speculation, the IC_{50} value of the test materials is expected to be higher against lymphocytes alone than against PBMC (lymphocytes + monocytes) leading to a higher selectivity for malignant THP-1 cells related to healthy lymphocytes. This theoretically higher SI, especially of compound **2b**, could exceed the targeted value of 10. **2b** but also **1a** and **2a** are therefore considered to be valuable candidates for the potential treatment of acute monocytic leukemia and should be further investigated *in vitro* using primary patient material. Moreover, *in vivo* experiments should be performed for safety and efficacy testing to clarify the impact of a treatment on healthy monocytic cells as simplified models of cancer cells and PBMC in culture cannot adequately model the complexity of the hematopoietic system as well as the human body. Based on the currently available literature, the compounds were not yet tested before against MV4-11 and THP-1 cell lines as well as PBMC as primary cell type since no previous study was found.

Cytotoxicity against adherent cells

Previously, polygodial and its derivatives were tested against the adherent cell lines MCF-7 (breast cancer), PC-3, and DU-145 (both prostate cancer) showing promising selectivity when comparing with non-malignant colon epithelial cells [29]. In the present study, non-malignant human gingival fibroblasts (GF) as well as the malignant cell lines Sk-Mel29 (malignant melanoma) and LN-229 (glioblastoma multiforme) were chosen for cytotoxicity analyses of the compounds. As stated before, the treatment with 1% Triton X-100 served as positive control for the maximum cell lysis effect to be reached by our test compounds. Except **1a** against GF, all test materials led to significantly reduced cell viabilities, whereby the effect was more pronounced against Sk-Mel29 and LN-229 than against GF (Fig. 3**A**) indicating a cell-type dependent cytotoxicity of the compounds.

Cell-type dependence could be confirmed by the SI values. Therefore, analogous to the previous section, the respective IC_{50} of the compound against Sk-Mel29 and LN-229 cell lines determined on the basis of their dose–response curves (Fig. 3**B**) were related to those against non-malignant GF. A SI value of >10 is the target for sufficient selectivity *in vitro* [28]. Sk-Mel29 and LN-229 cell lines showed similar dose-responses with IC_{50} values between 0.61 μg/mL (2.46 μM of compound **2b**) and 1.83 μg/mL (7.81 μM of compound **1a**) as well as between 0.68 μg/mL (2.74 μM of compound **2b**) and 5.25 μg/mL (22.40 μM of compound **1a**), respectively (Fig. 3, Table 3). In contrast, GF were the most robust cells in this study with IC_{50} values of at least 36.53 μg/mL (147.11 μM of compound **2b**). The respective SI values for Sk-Mel29 and LN-229 cells were > 10 up to about 60 indicating tumor-cell specificity. Thus, a local treatment of malignant melanoma and glioblastoma might be considered and further evaluated in subsequent *in vitro* and *in vivo* efficacy and safety studies.

The compound **2b** showed the highest toxicity towards all cell lines tested in this study followed by compound **2a**, while compound **1a** was less effective. This is consistent with results reported previously where **2a** exhibited an at least three-fold stronger inhibitory effect on the human tumor cell line KB (mouth epidermoid carcinoma) than **1a** [18]. These findings might be explained by the additional hydroxyl group at position C-9 in the molecule structure of **2a** and **2b**. Furthermore, the coloratane-type skeleton of **2b** seems to have a stronger impact on human cells than the drimane-type **2a** and **1a**. For further improvements, the coloratane skeleton might be the ideal target for structural modifications, such as oxo-functionalization of the exocyclic methylene group.

Effect on cell morphology

In the present study, swelling of hematopoietic cells, detachment, and rounding of adherent cells as well as partial or complete leakage of the cell content were observed when treated with the respective IC_{50} of the compounds (Fig. 4) indicating an increased cell permeability. This was also observed on **1a** and **2a** treated human cancer cells in previous studies [29,30]. It is already known, that **1a** acts as detergent on yeast cell membrane causing an increased permeability and leakage of cell components [31]. These observations provide another crucial hint that the cell membrane is the target site for the mode of action not only of **1a** but also of **2a** and **2b**.

Conclusion

Due to the high similarity of healthy/non-cancerous and malignant cells, the main challenge of cancer treatment is the distinction between these cells to minimize side effects. To highlight the great potential of the compounds **1a**, **2a**, and **2b** as selective anti-cancer drugs, we developed a model, which takes already known modes of action of the compounds, especially of **1a**, into account and explains why specific and relevant cancer cells and monocytes are more susceptible than healthy cells and lymphocytes, respectively (Fig. 5). As already mentioned, **1a** is known to target the cell membrane by acting as detergent [31], but the cell membrane is a non-specific rather than a specific target since it is present in every cell. However, different membrane fatty acid profiles were reported between healthy and malignant cells as well as between lymphocytes and monocytes [32]. For instance, primary monocytes were shown to have the highest content of mono- and polyunsaturated fatty acids compared to T and B lymphocytes, and also cancer cell lines were reported to exhibit a higher amount of monounsaturated fatty acids than their healthy primary counterparts [32]. It is conceivable that a specific membrane fatty acid profile present in monocytes and some cancer cells could lead to a stronger interaction with the compounds followed by membrane rupture and induction of necrosis. Polygodial is furthermore known to generate reactive oxygen species (ROS) [33] as

Table 2
Half-maximum inhibitory concentration (IC_{50}) of the compounds **1a**, **2a**, and **2b** against human peripheral blood mononuclear cells (PBMC) and human blood cancer cell lines MV4-11 and THP-1 as well as selectivity index (SI) related to PBMC.

	PBMC		MV4-11			THP-1		
	IC_{50}		IC_{50}		SI	IC_{50}		SI
Compound	μg/mL	μM	μg/mL	μM	–	μg/mL	μM	–
1a	2.55	10.88	1.62	6.91	1.57	0.52	2.22	4.90
2a	1.06	4.23	0.80	3.20	1.33	0.28	1.12	3.79
2b	0.71	2.86	0.65	2.62	1.09	0.11	0.44	6.45

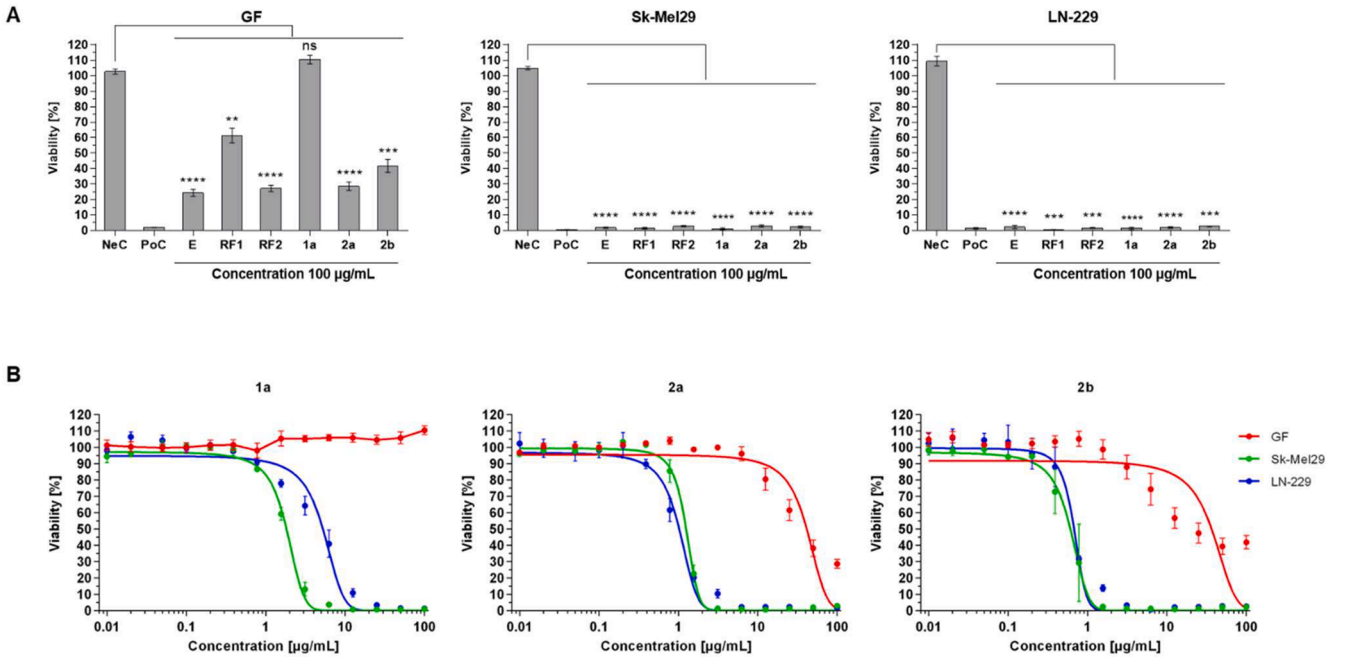

Fig. 3. Effects of *W. ugandensis* plant materials and its single compounds on the viability of human adherent cells. **A)** 100 µg/mL of the extract (E), relevant fractions 1 (RF1) and 2 (RF2), **1a**, **2a**, and **2b**, respectively, were tested against non-malignant human gingival fibroblasts (GF) as well as the cancer cell lines Sk-Mel29 and LN-229. 1% Triton X-100 was used as positive control (PoC) indicating complete cell lysis. Cell viabilities were compared to those of untreated cells (negative control, NeC) (ns: not statistically significant with $p > 0.05$; ** $p < 0.01$; *** $p < 0.001$; **** $p < 0.0001$ (unpaired *t*-test with/without Welch's correction)). **B)** Dose-response curves of **1a**, **2a**, and **2b** against GF, Sk-Mel29, and LN-229. Cell viabilities were normalized to viability of untreated cells. Non-linear regression was used to display sigmoidal curves of the cell viability allowing the determination of the respective half-maximum inhibitory concentration (IC_{50}). The experiments were performed in triplicates including three biological replicates with three technical replicates each, and the data are expressed as arithmetic mean ± standard error of the mean indicated by error bars.

Table 3
Half-maximum inhibitory concentration (IC_{50}) of the compounds **1a**, **2a**, and **2b** against human gingival fibroblasts (GF) and human cancer cell lines Sk-Mel29 and LN-229 as well as selectivity index (SI) related to GF.

	GF		Sk-Mel29			LN-229		
	IC_{50}		IC_{50}		SI	IC_{50}		SI
Compound	µg/mL	µM	µg/mL	µM	–	µg/mL	µM	–
1a	> 100[a]	> 426.75	1.83	7.81	> 54.64	5.25	22.40	> 19.05
2a	41.41	165.42	1.25	4.99	33.13	1.03	4.11	40.20
2b	36.53	147.11	0.61	2.46	59.89	0.68	2.74	53.72

[a] no inhibitory effect up to 100 µg/mL (426.75 µM).

well as to activate transient receptor potential vanilloid-1 (TRPV1) leading to an influx of calcium ions (Ca^{2+}) into the cells [34]. TRPV1 is mostly thought to be a pain receptor in neural cells but it is also expressed on monocytes, THP-1 cells, PBMC including T and natural killer cells as well as cancer cells [35–38]. Beside its localization on the cell surface, TRPV1 was also observed on mitochondria membrane of various human cells [39]. After entering the cytosol, activation of the mitochondrial TRPV1 by the compounds can lead to Ca^{2+} overload in the mitochondria inducing loss of mitochondrial membrane potential [39], which was already reported for **1a** [29]. Both, ROS and Ca^{2+} overload in the cell as well as in the mitochondria can trigger apoptosis [39–41]. During the initiation of necrosis caused by membrane rupture and/or apoptosis caused by ROS and Ca^{2+} overload, scramblase is activated to flip phosphatidylserine (PS) from the inner to the outer leaflet of the membrane, which is a signal for phagocytosis leading to cell death [42]. Generally, PS is completely absent on the outer cell membrane leaflet of healthy cells including lymphocytes, but it was shown that PS is already present in low levels on the outer surface of some cancer cells and monocytes [43,44]. Thus, cancer cells and monocytes are assumed to be more vulnerable to further PS addition on the surface triggered by cell membrane disruption, ROS and Ca^{2+} overload caused by **1a**, **2a**, and **2b**. Indeed, increasing ROS and Ca^{2+} levels can be a promising therapeutic strategy for the selective killing of cancer cells [45] such as acute monocytic leukemia, malignant melanoma and glioblastoma.

In summary, three sesquiterpenoids – polygodial **1a**, warburganal **2a**, and muzigadial **2b** – were efficiently isolated from *W. ugandensis* stem bark under mild conditions. Additionally, a new compound of *W. ugandensis* was identified as 9-deoxymuzigadial **1b**. Due to the observed hypersensitivity of monocytic cells, the compounds, especially **2b**, may represent valuable candidates to destroy monocytic leukemia cells with no or only small influence on other blood cells, such as lymphocytes. Furthermore, compared to solid cancer cell lines, a higher resistance of healthy fibroblasts against the sesquiterpenoids was observed, which may potentially provide a selective therapy approach, such as against malignant melanoma and glioblastoma multiforme. However, to be considered as therapeutically useful substances, further research on the compounds should be followed e.g. *in vivo* efficacy and safety studies as well as appropriate clinical trials. Another promising strategy is the use of polygodial, warburganal, and muzigadial as lead compounds for

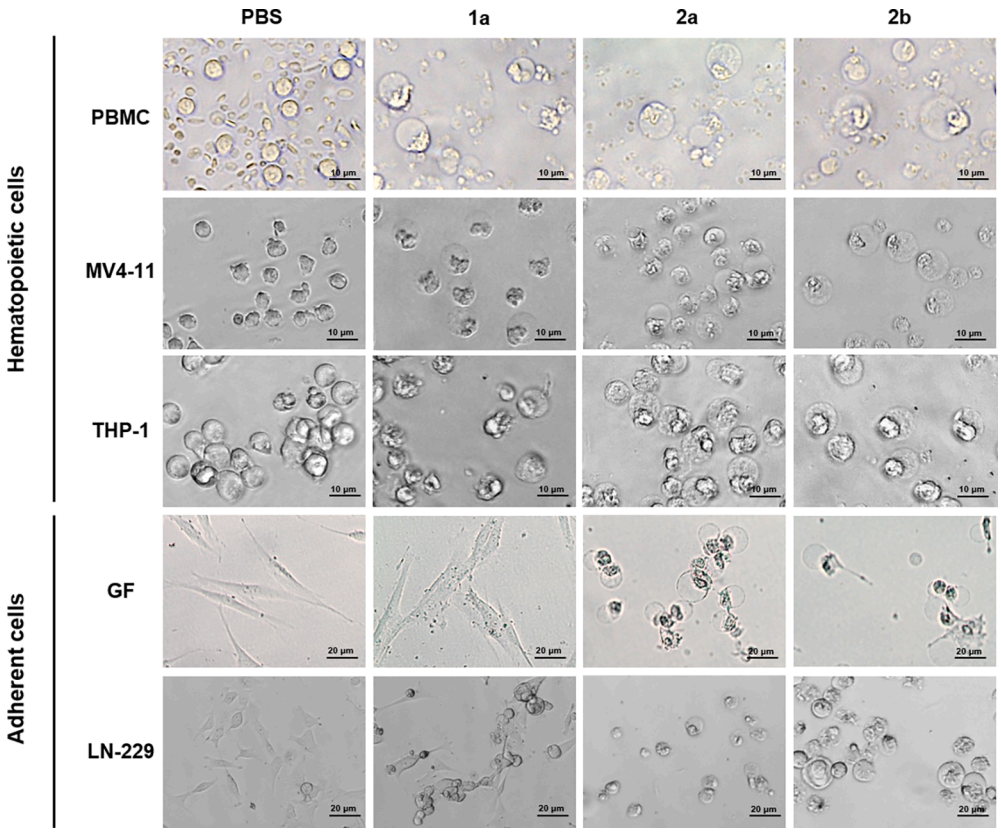

Fig. 4. Effects of the compounds **1a**, **2a**, and **2b** on the cell morphology of hematopoietic cells (peripheral blood mononuclear cells (PBMC), MV4-11, THP-1) as well as adherent cells (gingival fibroblasts (GF), LN-229) compared to untreated cells. At the respective IC_{50}, the compounds led to swelling of the cells in the case of hematopoietic cells, to detachment and rounding of adherent cells. The cell content had a rugged appearance and was either packed at the inner cell membrane or located partly or entirely outside the cell. As an exception, the treatment of GF with compound **1a** (100 µg/mL) had only small influence on cell morphology.

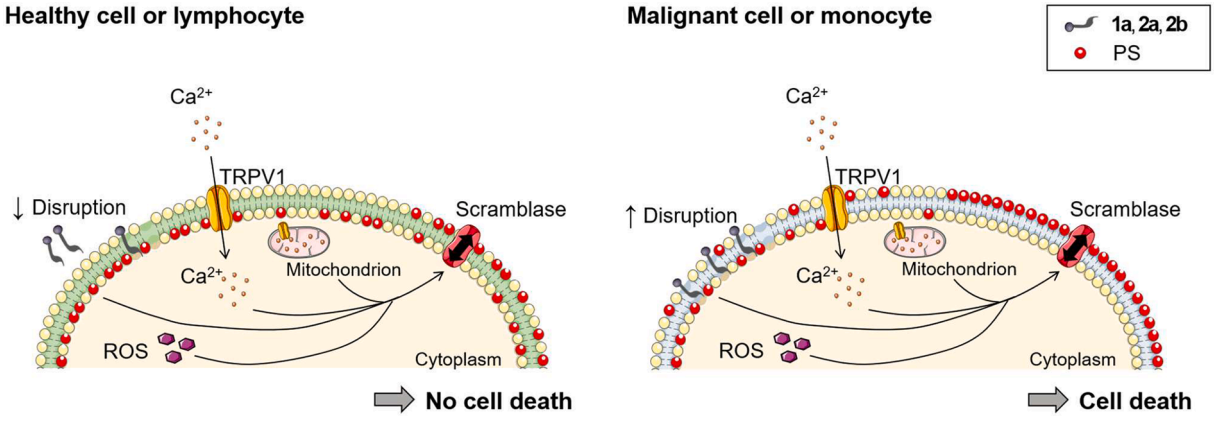

Fig. 5. Model of the mechanisms by which the compound **1a**, **2a**, and **2b** may lead to death of some cancer cells and monocytes compared to healthy cells and lymphocytes, respectively. The compounds **1a**, **2a**, and **2b** act as detergents causing cell membrane disruption and necrosis. Due to different membrane fatty acid profiles, they may stronger interact with the cell membrane of malignant cells and monocytes than of healthy cells and lymphocytes, respectively. Furthermore, they generate reactive oxygen species (ROS) and activate transient receptor potential vanilloid-1 (TRPV1) leading to an influx of calcium ions (Ca^{2+}) into the cells as well as mitochondria inducing apoptosis. As a result, scramblase is stimulated to flip phosphatidylserine (PS) from the inner to the outer leaflet of the membrane, which is a signal for phagocytosis leading to cell death. Since PS is intrinsically present on the surface of cancer cells and monocytes but not of healthy cells including lymphocytes, cancer cells and monocytes are assumed to be more susceptible to **1a**, **2a**, and **2b**. The figure was created with modified Servier Medical Art templates, licensed under a Creative Commons Attribution 3.0 Unported license: http://smart.servier.com.

further chemical modification in order to generate therapeutics with improved properties.

Experimental section

General experimental procedures

The isolation process is described in detail in Supporting Information (Fig. S2). GC–MS spectra of the compounds dissolved in dichloromethane (VWR International GmbH, Darmstadt, Germany) were recorded on Agilent 6890 N spectrometer combined with Agilent 5975B VL MSD detector. ESI-MS spectra were recorded in an ESI positive mode on the Bruker micrOTOF^{TM} mass spectrometer in deuterated chloroform ($CDCl_3$; VWR International GmbH, Darmstadt, Germany). Proton (^1H) NMR and carbon (^{13}C) NMR spectra were recorded on Varian Mercury Plus spectrometers (100 MHz, 400 MHz) in $CDCl_3$. Chemical shifts were reported in ppm (δ). For an exact allocation of the signals, 2D spectra (^1H, ^1H correlation spectroscopy, heteronuclear

multiple bond correlation) were involved in the structure analysis.

Plant material

The *W. ugandensis* stem bark material was collected from private plantations in Mutufu, Sironko District (Eastern Uganda) in August 2017 and exported in accordance with the International Plant Protection Convention 1951 and the Phytosanitary Convention for Africa 1971 (Licence/authority number: UQIS 00002931/93/PC (E); responsible person: Dr. Andreas Schubert, Fraunhofer IZI, Leipzig). The plants originated from the tree nursery of the National Forestry Resources Research Institute.

In silico investigations

Physicochemical and ADME properties were predicted and interpreted using the web tool SwissADME (available at http://www.swissadme.ch/) as it is described in detail in [26].

Cell lines

PBMC were obtained by density gradient centrifugation of blood from healthy donors (collected by the Institute for Transfusion Medicine of University Clinic of Leipzig, Germany and approved by the Ethics Committee of the Faculty of Medicine of the University Clinic of Leipzig, Germany, as no ethical or scientific concerns were raised (file reference number: 272-12-13082012)). PBMC, MV4-11 (DSMZ no.: ACC 102), THP-1 (DSMZ no.: ACC 16) and Sk-Mel29 (accession number: CVCL_6031; kindly provided by Prof. Dr. Barbara Seliger, University of Halle, Germany) were cultivated in RPMI 1640 medium + 10% FBS (both Gibco®, Thermo Fisher Scientific, Waltham, MA, USA). Human gingival fibroblasts (CLS 300703) were cultivated in DMEM/F12 (Gibco®) + 10% FBS. LN-229 (ATCC® CRL-2611; kindly provided by Prof. Dr. Frank Gaunitz, University Clinic of Leipzig, Germany) were cultivated in DMEM (Gibco®) + 10% FBS.

Resazurin-based cytotoxicity assay

To measure cell viability, alamarBlue™ cell viability reagent (Thermo Fisher Scientific, Waltham, MA, USA) was used. In preliminary tests, the length of reagent incubation time and cell number were determined for each cell line following the recommended procedure of the manufacturer (data not shown). 90 µL of cell suspension containing the respective cell number were filled into wells of a black flat bottom 96 well microplate (FLUOTRAC™, Greiner Bio-One International GmbH, Kremsmünster, Austria). Tissue growing cell lines were preincubated allowing the cells to adhere. 10 µL of the test material's solutions were added resulting in final concentrations between 0.01 µg/mL and 100 µg/mL, each with 0.5% DMSO. As positive control, 1% Triton™ X-100 (Merck KGaA, Darmstadt, Germany) with 0.5% DMSO was used. PBS (Gibco®) with 0.5 % DMSO was used as growth control. The respective cell medium without cells acted as blank. The plates were incubated at 37 °C and 5% CO_2. Depending on the results of the preliminary test, after 4–20 h, 10 µL of the cell viability reagent were added. The plates were further incubated at 37 °C and 5% CO_2 until 24 h total incubation time was reached. The emitted fluorescence was measured at 590 nm with an excitation wavelength of 530 nm using the Tecan Infinite® M200 microplate reader (Tecan Trading AG, Männedorf, Switzerland). The fluorescence intensity correlated directly to the number of viable cells in the culture. After subtracting the blank value from each value, the cell viability was normalized to untreated cells in the growth control.

Flow cytometry

PBMC distribution was analysed at BD FACSCanto™ II (Becton, Dickinson and Company, Franklin Lakes, NY, USA) after a 24 h incubation with the determined IC_{50} of the test materials. The following antibodies were used: FITC mouse anti-human CD3 (clone UCHT1; BD Pharmingen™), APC mouse anti-human CD19 (clone HIB19; BD Pharmingen™), PerCP mouse anti-human CD14 (clone MoP9; BD Biosciences) and PE-Cy7 mouse anti-human CD56 (clone NCAM16.2; BD Biosciences).

Statistics

Graph Pad Prism 6 software (GraphPad Software Inc., La Jolla, CA, USA) was used for all statistical analyses and the generation of the dose–response curves. The F test was performed to compare the variances of the data sets. For non-significantly different variances ($p > 0.2$), an unpaired *t*-test was performed, while an unpaired *t*-test with Welch's correction was used, if significantly different variances ($p < 0.2$) were determined. Probabilities of $p < 0.05$ were considered as statistically significant and are indicated by asterisks (* $p < 0.05$; ** $p < 0.01$; *** $p < 0.001$; **** $p < 0.0001$). To determine IC_{50} values, nonlinear regression of the dose–response curves was performed using the equation log (inhibitor) vs. response (normalized data) with variable slope (four parameters).

Author contributions

The manuscript was written through contributions of all authors. All authors have given approval to the final version of the manuscript.

Funding sources

This work was funded by the Fraunhofer Internal Programs under Grant No. MAVO 600806.

Declaration of Competing Interest

Andreas Schubert has patent #WO2011138334A1 issued to Fraunhofer Gesellschaft zur Förderung der Angewandten Forschung eV. Andreas Schubert declares that he is involved in a company that cultivates *Warburgia ugandensis* for human and animal healthcare applications.

Acknowledgement

We greatly thank our colleagues and collaboration partners from the Fraunhofer Cluster of Excellence Immune-Mediated Diseases CIMD as well as MAVO Synergy-Boost consortium including Fraunhofer Institute for Molecular Biology and Applied Ecology IME, Fraunhofer Institute for Toxicology and Experimental Medicine ITEM, and Fraunhofer Institute for Manufacturing Technology and Advanced Materials IFAM. We thank Prof. Dr. Barbara Seliger and Prof. Dr. Frank Gaunitz for providing the cell lines Sk-Mel29 and LN-229, respectively. Furthermore, we thank Dr. Maik Icker as well as Dr. Claudia Birkemeyer from the Institute of Analytical Chemistry of Leipzig University for providing the analytical tools for the compound identification.

Appendix A. Supplementary data

Overview of *W. ugandensis* compounds; detailed description of the isolation process; NMR and chromatographic data; *in silico* analysis; PBMC distribution after compound treatment (PDF)

Supplementary data to this article can be found online at https://doi.org/10.1016/j.rechem.2021.100242.

References

[1] WHO. *Ten threats to global health in 2019*. https://www.who.int/news-room/spotlight/ten-threats-to-global-health-in-2019 (accessed 2020-11-04).

[2] F. Bray, J. Ferlay, I. Soerjomataram, R.L. Siegel, L.A. Torre, A. Jemal, Global cancer statistics 2018: GLOBOCAN estimates of incidence and mortality worldwide for 36 cancers in 185 countries, CA: Cancer J. Clin. 68 (6) (2018) 394–424, https://doi.org/10.3322/caac.21492.

[3] J. Ferlay, M. Ervik, F. Lam, M. Colombet, L. Mery, M. Piñeros, A. Znaor, I. Soerjomataram, F. Bray, Global Cancer Observatory: Cancer Today. (2020).

[4] G.M. Cragg, D.J. Newman, Natural products: a continuing source of novel drug leads, BBA 1830 (6) (2013) 3670–3695, https://doi.org/10.1016/j.bbagen.2013.02.008.

[5] L.N. Silva, K.R. Zimmer, A.J. Macedo, D.S. Trentin, Plant natural products targeting bacterial virulence factors, Chem. Rev. 116 (16) (2016) 9162–9236, https://doi.org/10.1021/acs.chemrev.6b00184.

[6] A. Maroyi, The genus Warburgia: A review of its traditional uses and pharmacology, Pharm. Biol. 52 (3) (2014) 378–391, https://doi.org/10.3109/13880209.2013.837935.

[7] J.O. Abuto, A. Muchugi, D. Mburu, A.K. Machocho, G.M. Karau, Variation in Antimicrobial Activity of Warburgia ugandensis Extracts from Different Populations across the Kenyan Rift Valley, J. Microbiol. Res. (2016), https://doi.org/10.5923/j.microbiology.20160603.02.

[8] D. Olila, Olwa-Odyek, J. Opuda-Asibo, Antibacterial and antifungal activities of extracts of Zanthoxylum chalybeum and Warburgia ugandensis, Ugandan medicinal plants, African Health Sci. 1 (2) (2001) 66–72.

[9] Z.H. Mbwambo, P. Erasto, E. Innocent, P.J. Masimba, Antimicrobial and cytotoxic activities of fresh leaf extracts of Warburgia ugandensis, Tanzania J. Hlth Res. 11 (2) (2009), https://doi.org/10.4314/thrb.v11i2.45205.

[10] P.S. Were, P. Kinyanjui, M.M. Gicheru, E. Mwangi, H.S. Ozwara, Prophylactic and curative activities of extracts from Warburgia ugandensis Sprague (Canellaceae) and Zanthoxylum usambarense (Engl.) Kokwaro (Rutaceae) against Plasmodium knowlesi and Plasmodium berghei, J. Ethnopharmacol. 130 (1) (2010) 158–162, https://doi.org/10.1016/j.jep.2010.04.034.

[11] Ngure, Peter & Tonui, Willy & Ingonga, Johnstone & Mutai, Charles & Kigondu, Elizabeth & Ng, Zipporah & Rukunga, Geoffrey & Kimutai, Albert. In vitro antileishmanial activity of extracts of Warburgia ugandensis (Canellaceae), a Kenyan medicinal plant. *J. Med. Plants Res.* **2009**, *3*.

[12] M. Kuglerova, P. Marsik, T. Vanek, L. Kokoska, O. Wanyana-Maganyi, P. Van Damme, J. Grade, Antioxidative activity of ugandan medicinal plants, Afr. J. Tradit. Complement. Altern. Med. 6 (2009) 375–376.

[13] L.W. Karani, F.M. Tolo, S.M. Karanja, C. Khayeka−Wandabwa, Safety of Prunus africana and Warburgia ugandensis in asthma treatment, S. Afr. J. Bot. 88 (2013) 183–190, https://doi.org/10.1016/j.sajb.2013.07.007.

[14] D. Kioy, A.I. Gray, P.G. Waterman, A comparative study of the stem-bark drimane sesquiterpenes and leaf volatile oils of Warburgia ugandensis and W. Stuhlmannii, *Phytochemistry* 29 (11) (1990) 3535–3538, https://doi.org/10.1016/0031-9422(90)85270-P.

[15] I. Kubo, Antifungal sesquiterpene dialdehydes from the Warburgia plants and their synergists. In *Structure and Chemistry (Part D)*; Studies in Natural Products Chemistry, Elsevier (1995) 233–249, https://doi.org/10.1016/S1572-5995(05)80086-9.

[16] I. Kubo, I. Miura, M.J. Pettei, Y.-W Lee, F. Pilkiewicz, K. Nakanishi, Muzigadial and warburganal, potent antifungal antiyeast, and African army worm antifeedant agents, Tetrahedron Lett. 18 (52) (1977) 4553–4556, https://doi.org/10.1016/S0040-4039(01)83566-8.

[17] A.A. Wube, F. Bucar, S. Gibbons, K. Asres, Sesquiterpenes from Warburgia ugandensis and their antimycobacterial activity, Phytochemistry 66 (19) (2005) 2309–2315, https://doi.org/10.1016/j.phytochem.2005.07.018.

[18] M. Xu, M. Litaudon, S. Krief, M.-T. Martin, J. Kasenene, B. Kiremire, V. Dumontet, F. Guéritte, Ugandenial A, a new drimane-type sesquiterpenoid from Warburgia ugandensis, Molecules (Basel, Switzerland) 14 (10) (2009) 3844–3850, https://doi.org/10.3390/molecules14103844.

[20] M.S. Al-Said, S.M. El-Khawaja, F.S. El-Feraly, C.D. Hufford, 9-Deoxy drimane sesquiterpenes from Canella winterana, Phytochemistry 29 (3) (1990) 975–977, https://doi.org/10.1016/0031-9422(90)80059-P.

[21] K.A. Wayman, P.J. de Larsen, L. Larsen, C.E. Sansom, N.B. Perry, Chemotaxonomy of Pseudowintera: sesquiterpene dialdehyde variants are species markers, Phytochemistry 71 (7) (2010) 766–772. DOI: 10.1016/j.phytochem.2010.01.017. Published Online: Feb. 20, 2010.

[22] P.K. Ngure, Z. Ng'ang'a, J. Ingonga, G. Rukunga, W.K. Tonui, In Vivo Efficacy of Oral and Intraperitoneal Administration of Extracts of Warburgia Ugandensis (Canellaceae) in Experimental Treatment of Old World Cutaneous Leishmaniasis Caused by Leishmania Major, Afr. J. Tradit. Complement. Altern. Med. 6 (2) (2009) 207–212.

[23] T. Gonfa, A. Fisseha, A. Thangamani, Isolation, characterization and drug-likeness analysis of bioactive compounds from stem bark of Warburgia ugandensis Sprague, Chem. Data Collect. 29 (2020) 100535, https://doi.org/10.1016/j.cdc.2020.100535.

[24] J. Just, T.B. Jordan, B. Paull, A.C. Bissember, J.A. Smith, Practical isolation of polygodial from Tasmannia lanceolata: a viable scaffold for synthesis, Org. Biomol. Chem. 13 (46) (2015) 11200–11207, https://doi.org/10.1039/C5OB01573A.

[25] Q.-W. Zhang, L.-G. Lin, W.-C. Ye, Techniques for extraction and isolation of natural products: a comprehensive review, Chin. Med. 13 (2018) 20, https://doi.org/10.1186/s13020-018-0177-x.

[26] A. Daina, O. Michielin, V. Zoete, SwissADME: a free web tool to evaluate pharmacokinetics, drug-likeness and medicinal chemistry friendliness of small molecules, Sci. Rep. 7 (2017) 42717, https://doi.org/10.1038/srep42717.

[27] Eduarda Fratoni, Vanessa Duarte Claudino, Rosendo Augusto Yunes, Gilberto C. Franchi, Alexandre E. Nowill, Valdir Cechinel Filho, Franco Delle Monache, Angela Malheiros, Further drimane sesquiterpenes from Drimys brasiliensis stem barks with cytotoxic potential, Naunyn-Schmiedeberg's Arch. Pharmacol. 389 (7) (2016) 791–797, https://doi.org/10.1007/s00210-016-1241-7.

[28] L.J. McGaw, E.E. Elgorashi, J.N. Eloff, Cytotoxicity of African Medicinal Plants Against Normal Animal and Human Cells. In *Toxicological Survey of African Medicinal Plants*; Elsevier, 2014; pp 181–233. DOI: 10.1016/B978-0-12-800018-2.00008-X.

[29] I. Montenegro, G. Tomasoni, C. Bosio, N. Quiñones, A. Madrid, H. Carrasco, A. Olea, R. Martinez, M. Cuellar, J. Villena, Study on the cytotoxic activity of drimane sesquiterpenes and nordrimane compounds against cancer cell lines, Molecules (Basel, Switzerland) 19 (11) (2014) 18993–19006, https://doi.org/10.3390/molecules191118993.

[30] A. Forsby, E. Walum, O. Sterner, The effect of six sesquiterpenoid unsaturated dialdehydes on cell membrane permeability in human neuroblastoma SH-SY5Y cells, Chem. Biol. Interact. 84 (1) (1992) 85–95, https://doi.org/10.1016/0009-2797(92)90123-3.

[31] M. Taniguchi, Y. Yano, E. Tada, K. Ikenishi, S. Oi, H. Haraguchi, K. Hashimoto, I. Kubo, Mode of Action of Polygodial, an Antifungal Sesquiterpene Dialdehyde, Agric. Biol. Chem. 52 (6) (1988) 1409–1414, https://doi.org/10.1080/00021369.1988.10868863.

[32] P. Poggi, R. Mirabella, S. Neri, E. Assirelli, P. Dolzani, E. Mariani, P.C. Calder, A. Chatgilialoglu, Membrane fatty acid heterogeneity of leukocyte classes is altered during in vitro cultivation but can be restored with ad-hoc lipid supplementation, Lipids Health Dis. 14 (2015) 165, https://doi.org/10.1186/s12944-015-0166-3.

[33] K. Machida, T. Tanaka, M. Taniguchi, Depletion of glutathione as a cause of the promotive effects of polygodial, a sesquiterpene on the production of reactive oxygen species in Saccharomyces cerevisiae, J. Biosci. Bioeng. 88 (5) (1999) 526–530, https://doi.org/10.1016/S1389-1723(00)87670-7.

[34] E. André, B. Campi, M. Trevisani, J. Ferreira, A. Malheiros, R.A. Yunes, J.B. Calixto, P. Geppetti, Pharmacological characterisation of the plant sesquiterpenes polygodial and drimanial as vanilloid receptor agonists, Biochem. Pharmacol. 71 (8) (2006) 1248–1254. DOI: 10.1016/j.bcp.2005.12.030. Published Online: Feb. 2, 2006.

[35] D.A. Kunde, J. Yingchoncharoen, S. Jurković, D.P. Geraghty, TRPV1 mediates capsaicin-stimulated metabolic activity but not cell death or inhibition of interleukin-1β release in human THP-1 monocytes, Toxicol. Appl. Pharmacol. 2018 (360) (2018) 9–17, https://doi.org/10.1016/j.taap.2018.09.025. Published Online: Sep. 20.

[36] J.K. Bujak, D. Kosmala, I.M. Szopa, K. Majchrzak, P. Bednarczyk, Inflammation, Cancer and Immunity-Implication of TRPV1 Channel, Front. Oncol. 9 (2019) 1087. DOI: 10.3389/fonc.2019.01087. Published Online: Oct. 16, 2019.

[37] A.T. Billeter, N. Galbraith, S. Walker, C. Lawson, S.A. Gardner, H. Sarojini, S. Galandiuk, H.C. Polk, TRPA1 mediates the effects of hypothermia on the monocyte inflammatory response, Surgery 158 (3) (2015) 646–654. DOI: 10.1016/j.surg.2015.03.065. Published Online: Jun. 6, 2015.

[38] L.S. Premkumar, M. Bishnoi, Disease-related changes in TRPV1 expression and its implications for drug development, Curr. Top. Med. Chem. 11 (17) (2011) 2192–2209, https://doi.org/10.2174/156802611796904834.

[39] R. Juárez-Contreras, K.A. Méndez-Reséndiz, T. Rosenbaum, R. González-Ramírez, S.L. Morales-Lázaro, TRPV1 channel: a noxious signal transducer that affects mitochondrial function, Int. J. Mol. Sci. 21 (23) (2020). DOI: 10.3390/ijms21238882. Published Online: Nov. 24, 2020.

[40] H.G. Wang, N. Pathan, I.M. Ethell, S. Krajewski, Y. Yamaguchi, F. Shibasaki, F. McKeon, T. Bobo, T.F. Franke, J.C. Reed, Ca2+-induced apoptosis through calcineurin dephosphorylation of BAD 284 (1999) 339–343.

[41] H.U. Simon, A. Haj-Yehia, F. Levi-Schaffer, Role of reactive oxygen species (ROS) in apoptosis induction, Apoptosis : an International Journal on Programmed Cell Death 5 (5) (2000) 415–418, https://doi.org/10.1023/A:1009616228304.

[42] G.C. Brown, J.J. Neher, Eaten alive! Cell death by primary phagocytosis: 'phagoptosis'. *Trends in Biochemical Sciences* **2012**, *37* (8), 325–332. DOI: 10.1016/j.tibs.2012.05.002. Published Online: Jun. 7, 2012.

[43] A.B. Lioi, A.L.R. Rodriguez, N.T. Funderburg, Z. Feng, A. Weinberg, S.F. Sieg, Membrane damage and repair in primary monocytes exposed to human β-defensin-3. *Journal of Leukocyte Biology* **2012**, *92* (5), 1083–1091. DOI: 10.1189/jlb.0112046. Published Online: Jul. 26, 2012.

[44] B. Sharma, S.S. Kanwar, Phosphatidylserine: A cancer cell targeting biomarker. *Seminars in Cancer Biology* **2018**, *52* (Pt 1), 17–25. DOI: 10.1016/j.semcancer.2017.08.012. Published Online: Sep. 1, 2017.

[45] P.T. Schumacker, Reactive oxygen species in cancer cells: live by the sword, die by the sword, Cancer Cell 10 (3) (2006) 175–176, https://doi.org/10.1016/j.ccr.2006.08.015.

[46] Isao Kubo, Antifungal Sesquiterpene Dialdehydes from the Warburgia Plants and their Synergists, in: Atta-ur-Rahman (Ed.), Studies in Natural Products Chemistry 17, Elsevier Science B.V., 1995.

[47] Abuto, et al., Diversity in the Phytochemical Profiles of Warburgia ugandensis Sprague from Different Populations across the Kenyan Rift Valley, Journal of Pharmaceutical, Chemical and Biological Sciences 6 (1) (2018) 41–51.